INTERNATIONAL JOURNAL FOR NUMERICAL METHODS IN ENGINEERING, VOL. 36, 2123–2140 (1993)

ON A FINITE ELEMENT METHOD FOR DYNAMIC CONTACT/IMPACT PROBLEMS

ROBERT L. TAYLOR

Department of Civil Engineering, University of California at Berkeley, Berkeley, CA 94720, U.S.A.

PANAYIOTIS PAPADOPOULOS

Department of Mechanical Engineering, University of California at Berkeley, Berkeley, CA 94720, U.S.A.

SUMMARY

This paper addresses the formulation and discrete approximation of dynamic contact/impact initial-value problems. The continuous problem is presented in the context of non-linear kinematics. Standard semi-discrete time integrators are introduced and are shown to be unsuccessful in modelling the kinematic constraints imposed on the interacting bodies during persistent contact. A procedure that bypasses the aforementioned difficulty is proposed by means of a novel variational formulation. Numerical simulations are conducted and the results are reported and discussed.

1. INTRODUCTION

Mechanical contact is encountered whenever two or more bodies physically interact along their boundaries. Contact is of particular interest in numerous engineering applications ranging from metal forming and machine design to soil–structure and structure–structure interaction under dynamic excitation.

The non-linear character of contact boundary conditions allows for very few interesting problems to be solved analytically. Since the inception of the finite element method in the late 1950s, numerical solutions to contact problems have been intensively investigated by various researchers. Conry and Seireg[1] appear to be the first to treat contact as a quadratic programming problem, while Chan and Tuba[2] first introduced a general slideline methodology. Moreover, the works of Francavilla and Zienkiewicz[3] on a flexibility approach and Hughes *et al.*[4] on Lagrange multiplier methods significantly contributed to the development of robust finite element approximations, applicable to the simulation of large-scale problems.

This work is concerned with the time dimension of contact problems. By way of background, non-linear elastodynamics is briefly reviewed in Section 2. Section 3 addresses the two-body contact problem in the continuous setting, while Section 4 presents Lagrange multiplier and penalty formulations in space and semi-discrete integrators in time suitable for finite element approximations. Section 5 investigates standard second-order implicit time integrators of the Newmark family and their performance in modelling jump conditions in the kinematic fields (e.g. velocities and accelerations) of the interacting bodies. These integrators are shown to produce undesirable oscillatory solutions along the contact surface. In present practice, control of these oscillations is attempted by introducing artificial bulk viscocity for the compressive waves in each body. In the present work, the original Lagrange multiplier formulation of the two-body problem

0029–5981/93/122123–18$14.00

Received 10 October 1991
Revised 28 September 1992

is appropriately extended so as to eliminate this inconsistency. One- and two-dimensional numerical simulations are offered in Section 6 and demonstrate the significance of the proposed formulation.

2. NON-LINEAR ELASTODYNAMICS

In this section the initial-value problem of non-linear elastodynamics is briefly reviewed. To this end, a deformable body $\mathbf{B}$ is identified with an open set Ω in the R^3 linear space equipped with the standard basis $(\mathbf{E}_1, \mathbf{E}_2, \mathbf{E}_3)$. It follows that a typical material point of $\mathbf{B}$ is algebraically represented by vector co-ordinates $\mathbf{X} = (X_1, X_2, X_3)$ in the undeformed (reference) configuration. The boundary of the body, $\partial\Omega$, possesses a unique outer normal $\mathbf{N}$ at each of its points, provided it is sufficiently smooth (at least point-wise differentiable). Furthermore, assume that there exists an invertible mapping $\mathscr{X}$ defined as

$$\mathscr{X}: \Omega \times R_0^+ \mapsto R^3 \mid \mathbf{x} = \mathscr{X}(\mathbf{X}, t)$$

where $\mathbf{x}$ denotes the position of particle $\mathbf{X}$ in the deformed (current) configuration at a generic time t. The displacement field, $\mathbf{u}$, associated with the motion, is introduced according to

$$\mathbf{u}(\mathbf{X}, t) = \mathscr{X} - \mathbf{X}$$

and the deformation gradient, $\mathbf{F}$, as

$$\mathbf{F} = \frac{\partial \mathbf{x}}{\partial \mathbf{X}}$$

The strong form of the initial-value problem of non-linear elastodynamics is described by the following set of equations:

$$\nabla \cdot \mathbf{P} + \rho_0 \mathbf{b} = \rho_0 \ddot{\mathbf{u}} \quad \text{on } \Omega \times R_0^+ \tag{1}$$

$$\mathbf{u} = \bar{\mathbf{u}} \quad \text{on } \Gamma_u \times R_0^+ \tag{2}$$

$$\mathbf{N} \cdot \mathbf{P} = \bar{\mathbf{T}} \quad \text{on } \Gamma_t \times R_0^+ \tag{3}$$

$$\mathbf{u}(\mathbf{X}, 0) = \mathbf{u}_0(\mathbf{X}) \quad \text{on } \Omega \tag{4}$$

$$\dot{\mathbf{u}}(\mathbf{X}, 0) = \dot{\mathbf{u}}_0(\mathbf{X}) \quad \text{on } \Omega \tag{5}$$

In the above, $\mathbf{u}_0$ and $\dot{\mathbf{u}}_0$ denote the initial displacement and velocity fields of the body, respectively, while $\mathbf{P}$ is the first Piola–Kirchhoff stress tensor. Also, $\rho_0 = \rho_0(\mathbf{X})$ is the mass density in the reference state and Γ_u, Γ_t are the Dirichlet and Neumann portions of the boundary, on which boundary displacements, $\bar{\mathbf{u}}$, and surface tractions, $\bar{\mathbf{T}}$, are specified, respectively. Γ_u and Γ_t are mutually disjoint and

$$meas(\Gamma_u) \geqslant 0$$

A hyper-elastic constitutive assumption is made in the present context; thus,

$$\mathbf{P}(\mathbf{X}, t) = \rho_0 \frac{\partial W}{\partial \mathbf{F}} \tag{6}$$

where W is a strain energy functional, per unit mass, expressed in terms of some invariant measure of deformation. Equations (1–6) constitute *Problem* (P).

An integral counterpart of *Problem* (P) with reference to both the temporal and the spatial dimension can be stated by means of Hamilton's law of varying action,[5,6] as follows:

Problem (V)
For any given time interval $(t_i, t_f] \subset R^+$, find $\mathbf{u} \in \mathscr{U}$ such that

$$D_{\tilde{\mathbf{u}}} \int_{t_i}^{t_f} \int_{\Omega} [\tfrac{1}{2}\rho_0 \dot{\mathbf{u}}\cdot\dot{\mathbf{u}} - \rho_0 W(\mathbf{u})]\,\mathrm{d}V\mathrm{d}t + \int_{t_i}^{t_f}\int_{\Omega} \rho_0 \mathbf{b}\cdot\tilde{\mathbf{u}}\,\mathrm{d}V\mathrm{d}t$$

$$+ \int_{t_i}^{t_f}\int_{\Gamma_t} \bar{\mathbf{T}}\cdot\tilde{\mathbf{u}}\,\mathrm{d}\Gamma\,\mathrm{d}t - \left.\int_{\Omega} \rho_0 \dot{\mathbf{u}}\cdot\tilde{\mathbf{u}}\,\mathrm{d}\Omega\right]_{t_i}^{t_f} = 0 \quad \forall \tilde{\mathbf{u}} \in \mathscr{U}$$

In the above equation, $D_{\tilde{\mathbf{u}}}$ denotes the Gâteaux derivative in the direction of $\tilde{\mathbf{u}}$. Also, $\mathscr{U}$ is the space of kinematically admissible displacements for the given problem given by

$$\mathscr{U} = \{\mathbf{u} \in H^1(\Omega \times R_0^+) \mid \mathbf{u} = \bar{\mathbf{u}} \quad \text{on } \Gamma_u \times R_0^+,\ \mathbf{u}(\mathbf{X}, 0) = \mathbf{u}_0,\ \dot{\mathbf{u}}(\mathbf{X}, 0) = \dot{\mathbf{u}}_0 \text{ on } \Omega\}$$

while $\tilde{\mathscr{U}}$ is the associated space of admissible variations defined as

$$\tilde{\mathscr{U}} = \{\tilde{\mathbf{u}} \in H^1(\Omega \times R_0^+) \mid \tilde{\mathbf{u}} = \mathbf{0} \text{ on } \Gamma_u \times R_0^+,\ \tilde{\mathbf{u}}(\mathbf{X}, 0) = \mathbf{0},\ \dot{\tilde{\mathbf{u}}}(\mathbf{X}, 0) = \mathbf{0} \text{ on } \Omega\}$$

After integration by parts on the kinetic energy, Hamilton's law of varying action gives rise to a statement of virtual work for the initial-value problem according to

$$\int_{t_i}^{t_f} \left\{ \int_{\Omega} [\rho_0 \ddot{\mathbf{u}}\cdot\tilde{\mathbf{u}} + \rho_0 D_{\tilde{\mathbf{u}}} W(\mathbf{u}) - \rho_0 \mathbf{b}\cdot\tilde{\mathbf{u}}]\,\mathrm{d}V - \int_{\Gamma_t} \bar{\mathbf{T}}\cdot\tilde{\mathbf{u}}\,\mathrm{d}\Gamma \right\}\mathrm{d}t = 0 \quad \forall \tilde{\mathbf{u}} \in \tilde{\mathscr{U}},\ (t_i, t_f] \subset R^+ \quad (7)$$

Equation (7) constitutes the basis for the space–time discretization of the problem and will be subsequently utilized in the development of finite elements for dynamic contact.

3. DYNAMIC CONTACT PROBLEM

In this section a local formulation of the dynamic contact problem is furnished. Considerations are restricted to the two-body problem, with generalization to multi-body contact omitted for simplicity. Observing the notation of the previous section, the boundary of bodies $\mathbf{B}^1$ and $\mathbf{B}^2$ can be uniquely decomposed into three distinct regions according to

$$\partial\Omega^\alpha = \partial\Gamma_u^\alpha \cup \partial\Gamma_t^\alpha \cup C, \quad \alpha = 1, 2$$

where C is the common contact surface. Contact is said to occur if $\mathrm{meas}(C) > 0$. Gap and pressure functions can be defined along C, by means of projection of boundary points from one body onto the other,[7] as

$$g : (\partial\Omega^1 - \Gamma_u^1) \times (\partial\Omega^2 - \Gamma_u^2) \times R_0^+ \mapsto R_0^+ \mid g = g_{1\to 2}(t)$$

$$p : (\partial\Omega^1 - \Gamma_u^1) \times (\partial\Omega^2 - \Gamma_u^2) \times R_0^+ \mapsto R_0^- \mid p = p_{1\to 2}(t)$$

The dynamic contact problem distinguishes itself from the static in that the inequality constraint conditions hold not only for the displacements along the contacting surfaces but also for their rates. The impenetrability constraint may be expressed as

$$\{[\mathbf{X}_{P^2} + \mathbf{u}(\mathbf{X}_{P^2}, t)] - [\mathbf{X}_{P^1} + \mathbf{u}(\mathbf{X}_{P^1}, t)]\}\cdot\mathbf{n}_{P^1}(\mathbf{X}, t) = 0 \quad (8)$$

where $\mathbf{n}_{P^1} \equiv \mathbf{n}$ is the outer unit normal from body $\mathbf{B}^1$ in the current configuration. Time differentiation of (8) results in

$$[\dot{\mathbf{u}}(\mathbf{X}_{P^2}, t) - \dot{\mathbf{u}}(\mathbf{X}_{P^1}, t)]\cdot\mathbf{n}_{P^1}(\mathbf{X}, t) + \{[\mathbf{X}_{P^2} + \mathbf{u}(\mathbf{X}_{P^2}, t)] - [\mathbf{X}_{P^1} + \mathbf{u}(\mathbf{X}_{P^1}, t)]\}\cdot\dot{\mathbf{n}}_{P^1}(\mathbf{X}, t) = 0$$

which, taking into account that the unit normal, $\mathbf{n}_{P^1}$, is, by definition, parallel to the distance between the contacting points, can be readily shown to reduce to

$$[\dot{\mathbf{u}}(\mathbf{X}_{P^2}, t) - \dot{\mathbf{u}}(\mathbf{X}_{P^1}, t)] \cdot \mathbf{n}_{P^1}(\mathbf{X}, t) = 0 \tag{9}$$

see Figure 1. Likewise, a second time differentiation on (8) yields

$$[\ddot{\mathbf{u}}(\mathbf{X}_{P^2}, t) - \ddot{\mathbf{u}}(\mathbf{X}_{P^1}, t)] \cdot \mathbf{n}_{P^1}(\mathbf{X}, t) + [\dot{\mathbf{u}}(\mathbf{X}_{P^2}, t) - \dot{\mathbf{u}}(\mathbf{X}_{P^1}, t)] \cdot \dot{\mathbf{n}}_{P^1}(\mathbf{X}, t) = 0$$

In the above equation, the second term on the left-hand side quantifies the effect of relative motion of the contacting points in the direction tangent to $\mathbf{n}_{P^1}$. This term is negligible when such relative motions are small or contact occurs between relatively flat surfaces; it is ignored in the remainder of this work. Then

$$[\ddot{\mathbf{u}}(\mathbf{X}_{P^2}, t) - \ddot{\mathbf{u}}(\mathbf{X}_{P^1}, t)] \cdot \mathbf{n}_{P^1}(\mathbf{X}, t) = 0 \tag{10}$$

As it has been just illustrated in the continuous setting, equations (9) and (10) are obtained directly from the impenetrability condition and, therefore, do not represent additional constraints. They have been derived here because of their significance in discrete solutions.

In the case of persistent contact, the two-body problem is summarized as follows:

Problem (P_c):
Given state at time t_i for Ω^α, $\alpha = 1, 2$, solve (1)–(6) at interval $(t_i, t_f]$ subject to

$$pg = 0, \quad p \leqslant 0, \, g \geqslant 0 \text{ on } C$$

Integral formulations of the problem can be obtained by exploiting the statement of Hamilton's law (or, equivalently, the statement of virtual work) presented earlier in this section. A formulation based on Lagrange multipliers reads as follows:

Problem (V_L)
Find $(\mathbf{u}^1, \mathbf{u}^2, p) \in \mathscr{U}^1 \times \mathscr{U}^2 \times \mathscr{P}$ such that

$$\int_{t_i}^{t_f} \sum_{\alpha=1}^{2} \left\{ \int_{\Omega^\alpha} [\rho_0^\alpha \ddot{\mathbf{u}}^\alpha \cdot \tilde{\mathbf{u}}^\alpha + \rho_0^\alpha D_{\tilde{\mathbf{u}}^\alpha} W^\alpha(\mathbf{u}^\alpha) - \rho_0^\alpha \mathbf{b}^\alpha \cdot \tilde{\mathbf{u}}^\alpha] \, \mathrm{d}V \right.$$
$$\left. - \int_{\Gamma_t^\alpha} \bar{\mathbf{T}}^\alpha \cdot \tilde{\mathbf{u}}^\alpha \, \mathrm{d}\Gamma \right\} \mathrm{d}t + \int_{t_i}^{t_f} \int_C (\tilde{p} g + p \delta g) \, \mathrm{d}\Gamma \, \mathrm{d}t = 0$$
$$\forall (\tilde{\mathbf{u}}^1, \tilde{\mathbf{u}}^2, \tilde{p}) \in \tilde{\mathscr{U}}^1 \times \tilde{\mathscr{U}}^2 \times \tilde{\mathscr{P}}, (t_i, t_f] \subset R^+$$

The spaces of admissible and virtual displacements are as in the previous section, while the

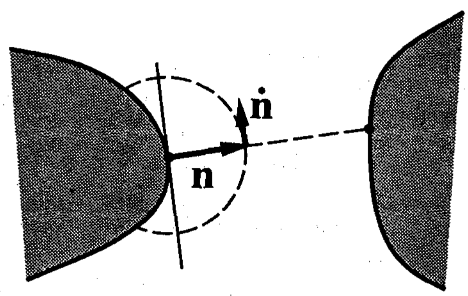

Figure 1. Contact conditions; the unit normal $\mathbf{n}$ and its time derivative

respective pressure fields is defined as

$$\mathscr{P} = \{p \in H^{-1/2}(C \times R_0^+) \mid p \leqslant 0\}$$

and

$$\tilde{\mathscr{P}} = \{\tilde{p} \in H^{-1/2}(C \times R_0^+) \mid \tilde{p} \leqslant 0\}$$

Formulations based on various penalty regularizations (in the classical penalty, perturbed Lagrangian or augmented Lagrangian sense) can also be obtained in a straightforward manner. Particularly, for the classical penalty method a weak formulation of the dynamic contact problem is stated as follows:

Problem (V_p):
Find$(\mathbf{u}^1, \mathbf{u}^2) \in \mathscr{U}^1 \times \mathscr{U}^2$ such that

$$\int_{t_i}^{t_f} \sum_{\alpha=1}^{2} \left\{ \int_{\Omega^\alpha} [\rho_0^\alpha \ddot{\mathbf{u}}^\alpha \cdot \tilde{\mathbf{u}}^\alpha + \rho_0^\alpha D_{\tilde{\mathbf{u}}^\alpha} W^\alpha(\mathbf{u}^\alpha) - \rho_0^\alpha \mathbf{b}^\alpha \cdot \tilde{\mathbf{u}}^\alpha] \, \mathrm{d}V \right.$$
$$\left. - \int_{\Gamma_t^\alpha} \bar{\mathbf{T}}^\alpha \cdot \tilde{\mathbf{u}}^\alpha \, \mathrm{d}\Gamma \right\} \mathrm{d}t + \int_{t_i}^{t_f} \int_C \varepsilon g \delta g \, \mathrm{d}\Gamma \, \mathrm{d}t = 0$$
$$\forall (\tilde{\mathbf{u}}^1, \tilde{\mathbf{u}}^2) \in \tilde{\mathscr{U}}^1 \times \tilde{\mathscr{U}}^2, (t_i, t_f] \subset R^+$$

Integral statements such as *Problem* (V_L) generally form the basis of finite element approximations to problems in elastodynamics. In this work, attention is focused on semi-discrete time integrators.

4. SPATIAL AND TEMPORAL DISCRETIZATION

In light of the above introduction, the domain discretization of the contacting bodies is achieved as in the static problem; for a given time, the displacement field, $\mathbf{u}$, and its rates are approximated according to

$$\begin{Bmatrix} \mathbf{u} \\ \dot{\mathbf{u}} \\ \ddot{\mathbf{u}} \end{Bmatrix} \approx \begin{Bmatrix} \mathbf{u}_h \\ \dot{\mathbf{u}}_h \\ \ddot{\mathbf{u}}_h \end{Bmatrix} = \mathbf{A}_{(I)}(\mathbf{X}) \begin{Bmatrix} \mathbf{u}_{(I)} \\ \mathbf{v}_{(I)} \\ \mathbf{a}_{(I)} \end{Bmatrix}$$

where $\mathbf{A}_{(I)}$ is a matrix of basis functions for the entire domain, normally composed by standard interpolation functions within each element (no summation is implied on I). Further, vectors $\mathbf{u}_{(I)}$, $\mathbf{v}_{(I)}$ and $\mathbf{a}_{(I)}$ consist of all nodal displacements, velocities and accelerations, respectively. In addition, the pressure field is spatially approximated according to

$$p \approx p_h = \mathbf{A}_{(I)}^p \mathbf{p}_{(I)}.$$

Moreover, subscript h characterizes spatially discretized fields. It follows that *Problem* (V_L) may be recast in the form:

Find $(\mathbf{u}_h^1, \mathbf{u}_h^2, p_h) \in \mathscr{U}_h^1 \times \mathscr{U}_h^2 \times \mathscr{P}_h$ such that

$$\int_{t_n}^{t_{n+1}} \sum_{\alpha=1}^{2} \{[\mathbf{M}^\alpha \mathbf{a}_{(I)}^\alpha + \mathbf{Q}^\alpha(\mathbf{u}_{(I)}^\alpha) - \mathbf{W}^\alpha + \mathbf{W}_\text{L}^\alpha(\mathbf{u}_{(I)}^\alpha)] \cdot \tilde{\mathbf{u}}_{(I)}^\alpha\} \, \mathrm{d}t + \int_{t_n}^{t_{n+1}} \mathbf{W}_p \tilde{\mathbf{p}}_{(I)} \, \mathrm{d}t = 0$$
$$\forall (\tilde{\mathbf{u}}_h^1, \tilde{\mathbf{u}}_h^2, \tilde{p}_h) \in \tilde{\mathscr{U}}_h^1 \times \tilde{\mathscr{U}}_h^2 \times \tilde{\mathscr{P}}_h, (t_n, t_{n+1}] \subset R^+$$

where

$$\mathbf{M}^\alpha = \sum_{\Omega_h^\alpha} \rho_0^\alpha \mathbf{A}_{(I)}^{\mathrm{T}} \mathbf{A}_{(I)}, \quad \mathbf{Q}^\alpha = \sum_{\Omega_h^\alpha} \nabla \mathbf{A}_{(I)}^{\mathrm{T}} \mathbf{P}(\mathbf{u}_{(I)}^\alpha)$$

$$\mathbf{W}^\alpha = \sum_{\Omega_h^\alpha} \rho_0^\alpha \mathbf{A}_{(I)}^{\mathrm{T}} \mathbf{b}^\alpha + \sum_{\Gamma_{th}^\alpha} \mathbf{A}_{(I)}^{\mathrm{T}} \bar{\mathbf{T}}^\alpha$$

$$\mathbf{W}_{\mathrm{L}}^\alpha = (-1)^\alpha \sum_{C_h} p_h \mathbf{A}_{(I)}^{\mathrm{T}} \mathbf{n}$$

and

$$\mathbf{W}_p = \sum_{C_h} g(\mathbf{U}_h) \mathbf{A}_{(I)}^{p\mathrm{T}}, \quad \alpha = 1, 2$$

In the above definitions, summation symbols over the domain or parts of its boundary refer to the usual assembly operation. Likewise, for the classical penalty formulation of *Problem* (V_{p}) the discrete problem takes the convenient form:

Find $(\mathbf{u}_h^1, \mathbf{u}_h^2) \in \mathscr{U}_h^1 \times \mathscr{U}_h^2$ such that

$$\int_{t_n}^{t_{n+1}} \sum_{\alpha=1}^{2} \{[\mathbf{M}^\alpha \mathbf{a}_{(I)}^\alpha + \mathbf{Q}^\alpha(\mathbf{u}_{(I)}^\alpha) - \mathbf{W}^\alpha + \mathbf{W}_\varepsilon^\alpha] \cdot \tilde{\mathbf{u}}_{(I)}^\alpha\} \, dt = 0$$

$$\forall (\tilde{\mathbf{u}}_h^1, \tilde{\mathbf{u}}_h^2) \in \tilde{\mathscr{U}}_h^1 \times \tilde{\mathscr{U}}_h^2, \ (t_n, t_{n+1}] \subset R^+,$$

where again

$$\mathbf{W}_\varepsilon^\alpha = (-1)^\alpha \sum_{C_h} \varepsilon g(\mathbf{U}_h) \mathbf{A}_{(I)}^{\mathrm{T}} \mathbf{n}$$

A Newmark scheme is employed for the time integration of the spatially discretized equations of motion resulting from the Lagrange multiplier or penalty formulation of the contact problem. The family of Newmark integrators, as originally suggested in Reference 8, imposes dynamic equilibrium at the two end points of the finite time interval $\Delta t_n \equiv t_{n+1} - t_n$. The general form of the integrator is

$$\mathbf{u}_{n+1} = \mathbf{u}_n + \mathbf{v}_n \Delta t_n + \tfrac{1}{2}[(1 - 2\beta)\mathbf{a}_n + 2\beta \mathbf{a}_{n+1}] \Delta t_n^2 \tag{11}$$

$$\mathbf{v}_{n+1} = \mathbf{v}_n + [(1 - \gamma)\mathbf{a}_n + \gamma \mathbf{a}_{n+1}] \Delta t_n \tag{12}$$

where $(\bullet)_n \equiv (\bullet)(t_n)$. Parameters β and γ (called the *Newmark parameters*) may vary according to

$$0 \leqslant \beta \leqslant 0{\cdot}5, \quad 0 \leqslant \gamma \leqslant 1$$

The overall characteristics of any particular Newmark scheme are governed by the choice of the above two parameters. In particular, unconditional stability is guaranteed for $2\beta \geqslant \gamma \geqslant 0{\cdot}5$, as shown in Reference 9. Furthermore, integration is globally first-order accurate (error $O(\Delta t^2)$) provided that $\gamma = 0{\cdot}5$.

For the remainder of this section, all subscripts associated with the spatial discretization of the various fields will be dropped in favour of those pertaining to the temporal description. The Lagrange multiplier formulation of the previous section leads to equations of motion written, at time t_{n+1}, as

$$\sum_{\alpha=1}^{2} [\mathbf{M}^\alpha \mathbf{a}_{n+1}^\alpha + \mathbf{Q}^\alpha(\mathbf{u}_{n+1}) - \mathbf{W}_{n+1}^\alpha + \mathbf{W}_L^\alpha(\mathbf{u}_{n+1}^\alpha)] = \mathbf{0} \tag{13}$$

$$g(\mathbf{u}_{n+1}^1, \mathbf{u}_{n+1}^2) = 0 \tag{14}$$

Use of equations (11) and (12) in (13) results in the elimination of the unknown velocity and acceleration fields, thus yielding a set of equations with the displacement vector at time t_{n+1} as the only unknown, according to

$$\sum_{\alpha=1}^{2}\left\{\frac{1}{\beta\,\Delta t_n^2}\mathbf{M}^\alpha\mathbf{u}_{n+1}^\alpha+\mathbf{Q}^\alpha(\mathbf{u}_{n+1}^\alpha)+\mathbf{W}_L^\alpha(\mathbf{u}_{n+1}^\alpha)-\mathbf{W}_{n+1}^\alpha\right.$$
$$\left.-\mathbf{M}^\alpha\frac{1}{\beta}\left[\frac{1}{\Delta t_n^2}\mathbf{u}_n^\alpha+\frac{1}{\Delta t_n}\mathbf{v}_n^\alpha+\frac{(1-2\beta)}{2}\mathbf{a}_n^\alpha\right]\right\}=\mathbf{0} \tag{15}$$

Similarly, the penalty formulation obtained in the previous section is easily discretized in time to produce a set of equations in terms of the displacements at t_{n+1} that read

$$\sum_{\alpha=1}^{2}\left\{\frac{1}{\beta\Delta t_n^2}\mathbf{M}^\alpha\mathbf{u}_{n+1}^\alpha+\mathbf{Q}^\alpha(\mathbf{u}_{n+1}^\alpha)+\mathbf{W}_\varepsilon^\alpha(\mathbf{u}_{n+1}^\alpha)-\mathbf{W}_{n+1}^\alpha\right.$$
$$\left.-\mathbf{M}^\alpha\frac{1}{\beta}\left[\frac{1}{\Delta t_n^2}\mathbf{u}_n^\alpha+\frac{1}{\Delta t_n}\mathbf{v}_n^\alpha+\frac{(1-2\beta)}{2}\mathbf{a}_n^\alpha\right]\right\}=\mathbf{0} \tag{16}$$

Equations (14)–(16) are generally non-linear and have to be solved by an iterative algorithm such as Newton's method or any of its variants.

5. DYNAMIC CONTACT/RELEASE CONDITIONS

In the preceding section, Newmark integrators were employed in the solution of the two-body contact problem, where contact/release constraints were imposed on the displacement fields, in accordance with (8). Unfortunately, in contrast with the continuous case, the velocity and acceleration fields recovered from such an integration scheme do not satisfy the respective rate impenetrability constraints realized by (9) and (10). This can be easily seen with the help of a simple example: consider a contact between two nodal points, each belonging to one of the contacting bodies. The points come into initial contact at time t_n and the following conditions hold:

$$\mathbf{X}^1+\mathbf{u}_n^1=\mathbf{X}^2+\mathbf{u}_n^2=\mathbf{0}$$
$$\mathbf{v}_n^1=\mathbf{v}_0,\quad \mathbf{v}_n^2=\mathbf{0}$$
$$\mathbf{a}_n^1=\mathbf{a}_n^2=\mathbf{0}$$

Enforcement of the impenetrability condition on the discrete displacement fields, as defined in (11), along the normal, $\mathbf{n}$, to the contact surface at time t_{n+1}, yields

$$(\mathbf{X}^1+\mathbf{u}_n^1)\cdot\mathbf{n}+\Delta t_n\mathbf{v}_n^1\cdot\mathbf{n}+\tfrac{1}{2}\Delta t_n^2[(1-2\beta)\mathbf{a}_n^1+2\beta\mathbf{a}_{n+1}^1]\cdot\mathbf{n}$$
$$=(\mathbf{X}^2+\mathbf{u}_n^2)\cdot\mathbf{n}+\Delta t_n\mathbf{v}_n^2\cdot\mathbf{n}+\tfrac{1}{2}\Delta t_n^2[(1-2\beta)\mathbf{a}_n^2+2\beta\mathbf{a}_{n+1}^2]\cdot\mathbf{n}$$

or, taking into account the conditions at t_n,

$$(\mathbf{a}_{n+1}^2-\mathbf{a}_{n+1}^1)\cdot\mathbf{n}=\frac{1}{\beta\,\Delta t_n}\mathbf{v}_0\cdot\mathbf{n} \tag{17}$$

provided that $\beta>0$. Likewise, substracting the discrete velocities of the two nodes at t_{n+1} from one another and using again the initial conditions at t_n gives

$$(\mathbf{v}_{n+1}^2-\mathbf{v}_{n+1}^1)\cdot\mathbf{n}=\gamma\,\Delta t_n(\mathbf{a}_{n+1}^2-\mathbf{a}_{n+1}^1)\cdot\mathbf{n}-\mathbf{v}_0\cdot\mathbf{n}$$

which, with the aid of (17), results in

$$(\mathbf{v}_{n+1}^2 - \mathbf{v}_{n+1}^1)\cdot\mathbf{n} = \left(\frac{\gamma}{\beta} - 1\right)\mathbf{v}_0\cdot\mathbf{n} \tag{18}$$

Equations (17) and (18) illustrate the problematic behaviour of Newmark integrators, when directly used in simulating dynamic contact/release conditions. It can be readily concluded that the discontinuity in the post-contact velocities is independent of the time step, while the discontinuity in the accelerations is inversely proportional to the time step; thus, consistency is not attained at $\Delta t \to 0$. Finally, notice that equations (17) and (18) were obtained without any reference to dynamic equilibrium (which, in this case, would only determine the exact position of the nodes at time t_{n+1}).

The above analysis indicates that a special treatment is necessary for an accurate simulation of contact/release conditions. Indeed, the discrepancy in the computed rate quantities, although immaterial within linear elasticity, can be potentially devastating in non-linear problems employing rate-dependent constitutive assumptions. In an earlier attempt, Hughes and co-workers have used the Newmark solution as a predictor to be subsequently followed by a corrector step, in which velocities were matched on the contact surface by means of a local wave propagation analysis. Moreover, accelerations were weighted by the (lumped) masses of the interacting nodes, so that dynamic equilibrium be observed after the treatment.[4] Here a slightly different methodology is proposed based on *a priori* satisfaction of the impenetrability constraint and its two rate forms, corresponding to equations (8), (9) and (10), respectively. To this end, the Lagrange multiplier formulation in Section 3 is augmented by the variational terms

$$\int_{C_h} \sum_{\alpha=1}^{2} \{ w_{\mathrm{v}}^{\alpha}[\mathbf{u}_{n+1}^{\alpha} - \mathbf{u}_n^{\alpha} - \Delta t_n \mathbf{v}_n^{\alpha} - \Delta t_n^2(\tfrac{1}{2} - \beta)\mathbf{a}_n^{\alpha} - \Delta t_n^2 \beta \mathbf{a}_{n+1}^{\alpha}]\cdot\mathbf{n}(\tilde{\mathbf{v}}_{n+1}^{\alpha}\cdot\mathbf{n}) + \lambda_{\mathrm{v}}(-1)^{\alpha}\tilde{\mathbf{v}}_{n+1}^{\alpha}\cdot\mathbf{n} + \tilde{\lambda}_{\mathrm{v}}(-1)^{\alpha}\mathbf{v}_{n+1}^{\alpha}\cdot\mathbf{n}\}\,\mathrm{d}\Gamma = 0 \tag{19}$$

and

$$\int_{C_h} \sum_{\alpha=1}^{2} \{ w_{\mathrm{a}}^{\alpha}[\mathbf{v}_{n+1}^{\alpha} - \mathbf{v}_n^{\alpha} - \Delta t_n(1-\gamma)\mathbf{a}_n^{\alpha} - \Delta t_n \gamma \mathbf{a}_{n+1}^{\alpha}]\cdot\mathbf{n}(\tilde{\mathbf{a}}_{n+1}^{\alpha}\cdot\mathbf{n}) + \lambda_{\mathrm{a}}(-1)^{\alpha}\tilde{\mathbf{a}}_{n+1}^{\alpha}\cdot\mathbf{n} + \tilde{\lambda}_{\mathrm{a}}(-1)^{\alpha}\mathbf{a}_{n+1}^{\alpha}\cdot\mathbf{n}\}\,\mathrm{d}\Gamma = 0 \tag{20}$$

where $w_{\mathrm{v}}^{\alpha}, w_{\mathrm{a}}^{\alpha} > 0$ are weighting functions. Equations (19) and (20) reveal that the Newmark integrator is modified along the contact boundary. Particularly, the admissible contact velocity and acceleration fields are, in principle, assumed independent of the displacements, while the Lagrange multipliers λ_{v} and λ_{a} enforce the conditions

$$[\![\mathbf{v}_{n+1}]\!]_{\mathrm{c}} = 0, \quad [\![\mathbf{a}_{n+1}]\!]_{\mathrm{c}} = 0$$

where

$$[\![(\bullet)]\!]_{\mathrm{c}} \equiv [(\bullet)^2 - (\bullet)^1]\cdot\mathbf{n}$$

The multipliers λ_{v} and λ_{a} are viewed as generalized momenta, energy conjugate to the contact velocities and accelerations, respectively. Equations (19) require that

$$w_{\mathrm{v}}^1[\mathbf{u}_{n+1}^1 - \mathbf{u}_n^1 - \Delta t_n \mathbf{v}_n^1 - \Delta t_n^2(\tfrac{1}{2} - \beta)\mathbf{a}_n^1 - \Delta t_n^2 \beta \mathbf{a}_{n+1}^1]\cdot\mathbf{n} - \lambda_{\mathrm{v}} = 0$$

and

$$w_{\mathrm{v}}^2[\mathbf{u}_{n+1}^2 - \mathbf{u}_n^2 - \Delta t_n \mathbf{v}_n^2 - \Delta t_n^2(\tfrac{1}{2} - \beta)\mathbf{a}_n^2 - \Delta t_n^2 \beta \mathbf{a}_{n+1}^2]\cdot\mathbf{n} + \lambda_{\mathrm{v}} = 0$$

along C_h. Premultiplying each of the above with the weighting function of the other, recalling that

$$[\![\mathbf{X} + \mathbf{u}_{n+1}]\!]_c = 0$$

and, finally, differencing, gives

$$\lambda_v = \frac{[\![\mathbf{X} + \mathbf{u}_n]\!]_c + \Delta t_n [\![\mathbf{v}_n]\!]_c + \Delta t_n^2(\frac{1}{2} - \beta)[\![\mathbf{a}_n]\!]_c}{1/w_v^1 + 1/w_v^2} \tag{21}$$

Similarly, equations (20) dictate that

$$w_a^1[\mathbf{v}_{n+1}^1 - \mathbf{v}_n^1 - \Delta t_n(1-\gamma)\mathbf{a}_n^1 - \Delta t_n \gamma \mathbf{a}_{n+1}^1]\cdot\mathbf{n} - \lambda_a = 0$$

and

$$w_a^2[\mathbf{v}_{n+1}^2 - \mathbf{v}_n^2 - \Delta t_n(1-\gamma)\mathbf{a}_n^2 - \Delta t_n \gamma \mathbf{a}_{n+1}^2]\cdot\mathbf{n} + \lambda_a = 0$$

Repeating the same process as before yields

$$\lambda_a = \frac{[\![\mathbf{v}_n]\!]_c + \Delta t_n(1-\gamma)[\![\mathbf{a}_n]\!]_c}{1/w_a^1 + 1/w_a^2} \tag{22}$$

In case one of the contacting bodies is rigid, then it is, by assumption, associated with infinite weighting functions, so that (21) and (22) are modified accordingly. Velocity and acceleration fields normal to the contact surface are recovered with the aid of the above constraint equations as

$$\mathbf{v}_{n+1}^\alpha\cdot\mathbf{n} = [\mathbf{v}_n^\alpha + \Delta t_n(1-\gamma)\mathbf{a}_n^\alpha + \Delta t_n\gamma\mathbf{a}_{n+1}^\alpha]\cdot\mathbf{n} - (-1)^\alpha\frac{\lambda_\alpha}{w_a^\alpha}$$

and

$$\mathbf{a}_{n+1}^\alpha\cdot\mathbf{n} = \frac{1}{\beta\Delta t_n^2}\left\{[\mathbf{u}_{n+1}^\alpha - \mathbf{u}_n^\alpha - \Delta t_n\mathbf{v}_n^\alpha - \Delta t_n^2(\tfrac{1}{2}-\beta)\mathbf{a}_n^\alpha]\cdot\mathbf{n} + (-1)^\alpha\frac{\lambda_v}{w_v^\alpha}\right\}$$

In the absence of contact, as well as during persistent contact, the proposed treatment reduces naturally to the associated Newmark method. Indeed, in the former case, as $meas(C_h) = 0$, all Lagrange multipliers disappear at the outset while, in the latter, equations (21) and (22) require the multipliers to be again identically equal to zero.

The weighting functions, w_v^α and w_a^α, are chosen so that the integrands in (19) and (20) be (virtual) work quantities. Here, they are set to be

$$w_v^\alpha(t) = \frac{m^\alpha}{\Delta t_n},\quad w_a^\alpha(t) = m^\alpha\Delta t_n,\quad t\in(t_n, t_{n+1}]$$

where m^α denotes a generalized characteristic mass quantity for body α.

Whenever release is detected (as defined in Reference 4), equations (19) and (20) yield, in direct analogy with initiation of contact,

$$[\![\mathbf{u}_{n+1}]\!]_c - \Delta t_n^2\beta[\![\mathbf{a}_{n+1}]\!]_c + \lambda_v\left(\frac{1}{w_v^1} + \frac{1}{w_v^2}\right) = 0 \tag{23}$$

and

$$[\![\mathbf{v}_{n+1}]\!]_c - \Delta t_n\gamma[\![\mathbf{a}_{n+1}]\!]_c + \lambda_a\left(\frac{1}{w_a^1} + \frac{1}{w_a^2}\right) = 0 \tag{24}$$

In this work, both Lagrange multipliers in (23) and (24) are set to be zero at release, as their appearance was originally identified with the (currently inactive) constraint of equal velocities and accelerations in the direction normal to the contact surface.

6. NUMERICAL SIMULATIONS

Numerical solutions of some dynamic contact/impact problems are presented in this section. Attention is focused on both kinematic and dual variables computed by the finite element method. Relatively simple one- and two-dimensional simulations are performed, as the modification to the Newmark integrators suggested in Section 5 is currently available only for node-to-node slidelines. The algorithm is incorporated within the environment of the fully non-linear general purpose Finite Element Analysis Program (FEAP), briefly documented in Chapter 15 of Reference 10 and Chapter 16 of Reference 11.

Although implicit time integration schemes are used throughout, an attempt is made to keep the time step as close to optimal, with regard to the explicit stability limit, as possible. Recall that the stability limit (or *Courant limit*) is generally defined as

$$s = \frac{c}{l}\Delta t \tag{25}$$

where c is the wave speed (depending on the type of waves developing in the actual problem), Δt is the discrete time step used in the integration and l is a characteristic spatial dimension of the discretization (e.g. mean element length in one-dimensional problems or mean element diameter in multi-dimensional problems).

All numerical simulations employ a standard Lagrange multiplier formulation in enforcing impenetrability. An exterior penalty formulation is also applicable as outlined in Section 3 without any algorithmic complications. Diagonal (lumped) mass matrices are used for all types of elements, as their behaviour is considered superior to that of the corresponding consistent matrices whenever, as in given class of problems, the associated kinematic fields exhibit discontinuities (or near-discontinuities) in time. Lumped masses are also used as weighting functions of the modified Newmark impact treatment.

6.1. Impact of bar on rigid wall

An elastic bar of Young's modulus E, cross-sectional area A and mass density ρ is travelling with constant velocity $\mathbf{v} = 1{\cdot}0\mathbf{E}_1$, when it impacts on a rigid wall at time $t = 0$, see Figure 2. The bar is modelled by two-node, one-dimensional linear elastic elements. The properties of the bar are chosen to be

$$E = 1{\cdot}0, \quad \rho = 1{\cdot}0, \quad A = 1{\cdot}0$$

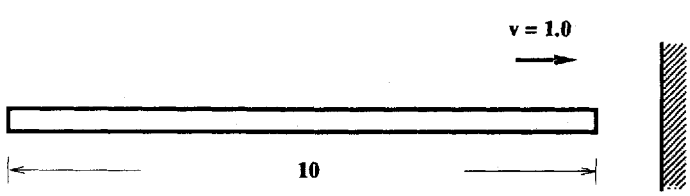

Figure 2. Bar on rigid wall

Gravity effects are not considered. A uniform mesh of 100 elements is considered and the time step is set to $\Delta t = 0{\cdot}1$.

Both classical and modified Newmark integrators are tested, with parameters $\beta = 0{\cdot}25$ and $\gamma = 0{\cdot}5$. Velocities and accelerations at the impacting tip of the bar are plotted in Figures 3 and 4, respectively, for the actual duration of contact. It is observed that classical Newmark integration results in highly oscillatory fields, while the proposed modification completely bypasses the problem.

Displacements, velocities and accelerations are also computed for time $t = 5$, at which the wave has reached the middle of the bar, see Figures 5 and 6. These computations are conducted with two distinctly different choices of the Newmark parameters, namely $\beta = 0{\cdot}25$, $\gamma = 0{\cdot}5$ (as before) and also $\beta = 0{\cdot}001$, $\gamma = 0{\cdot}5$. The latter choice corresponds to an almost explicit method, which, as expected, gives results superior to the former and, thus, will be employed for the remainder of the bar simulations.

6.2. *Impact of identical bars*

Two identical bars, one initially stationary and the other moving with constant velocity $\mathbf{v} = 1{\cdot}0\mathbf{E}_1$, contact each other at time $t = 0$, see Figure 7. All material and geometric properties of the bars, the domain discretization for each of them, as well as the Newmark parameters and time step are as in the previous problem. Figure 8 displays the history of displacements, velocities and forces for the contacting bar tips. The results are compared with the exact solution and are found to be very accurate. Local oscillations in the velocity at the time of wave reflections are noticed. Hughes *et al.*[4] proposes to eliminate them by introducing numerical dissipation (i.e. by increasing the value of γ).

6.3. *Impact of dissimilar bars*

Two bars of lengths and initial velocities as in Figure 7 come into contact at time $t = 0$. With reference to the same figure, the properties of the two bars are:

$$\text{Bar 1: } E = 0{\cdot}49, \quad \rho = 1{\cdot}0, \quad A = 1{\cdot}0$$

$$\text{Bar 2: } E = 1{\cdot}0, \quad \rho = 1{\cdot}0, \quad A = 1{\cdot}0$$

Bar 1 is discretized uniformly by 100 elements and Bar 2 by 70 elements, so that, for time step $\Delta t = 0{\cdot}142857$, both are integrated in time optimally (i.e. $s = 1$). Plots of the displacements, velocities and contact force at the contacting tip are shown in Figure 9. Excellent agreement with the exact solutions is exhibited for all three fields.

6.4. *Impact of identical spheres*

Two identical elastic spheres of radius $R = 8$ and initial distance between their centers of $d = 20$ travel collinearly with equal and opposite velocities of magnitude $\|\mathbf{v}\| = 1$, and, thus, collide at time $t = 2$. No gravity effects are included in the analysis. The spheres are modelled by axisymmetric nine-node bi-quadratic elements and the undeformed mesh is shown in Figure 10. The elastic constants for the spheres are

$$E_s = 5\cdot \times 10^2, \quad \nu_s = 0{\cdot}3$$

and two values of the mass density are considered, namely $\rho = 1{\cdot}0$ and $0{\cdot}001$. The Newmark parameters are set to $\beta = 0{\cdot}25$ and $\gamma = 0{\cdot}5$. The history of total force developed due to contact is

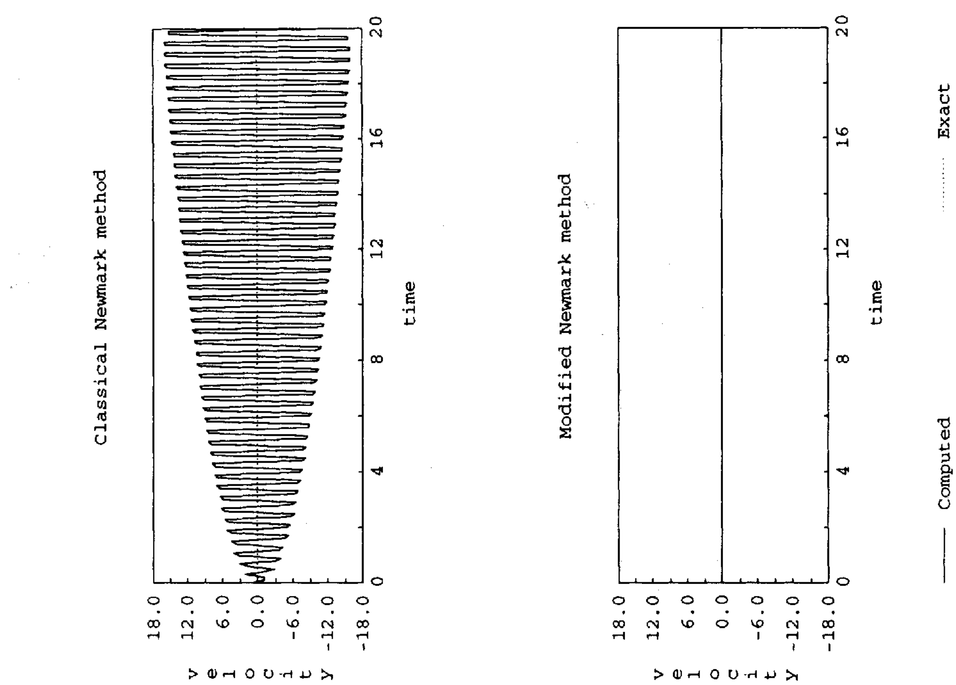

Figure 3. Bar on rigid wall; velocity at impact point

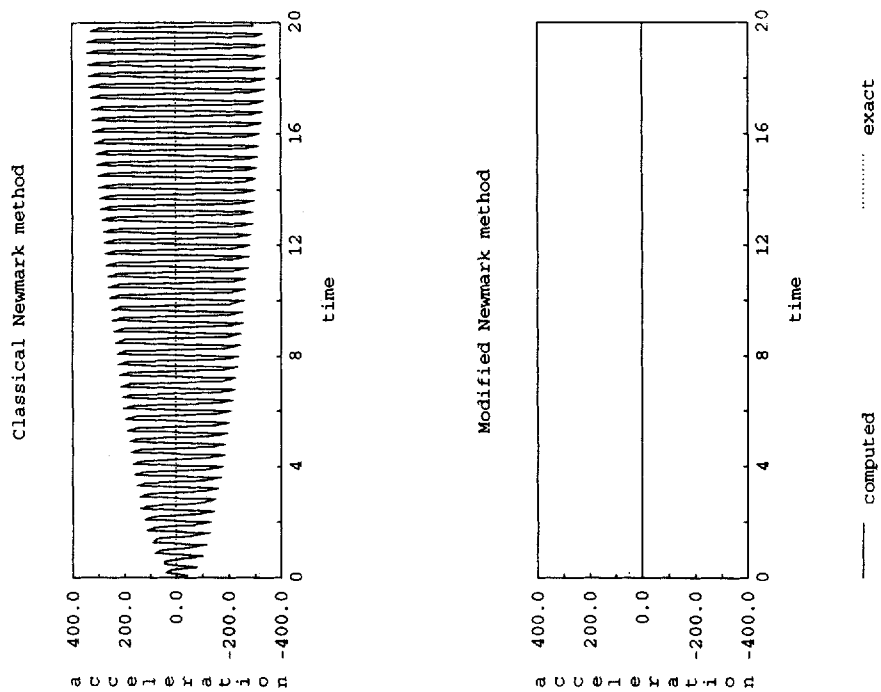

Figure 4. Bar on rigid wall; acceleration at impact point

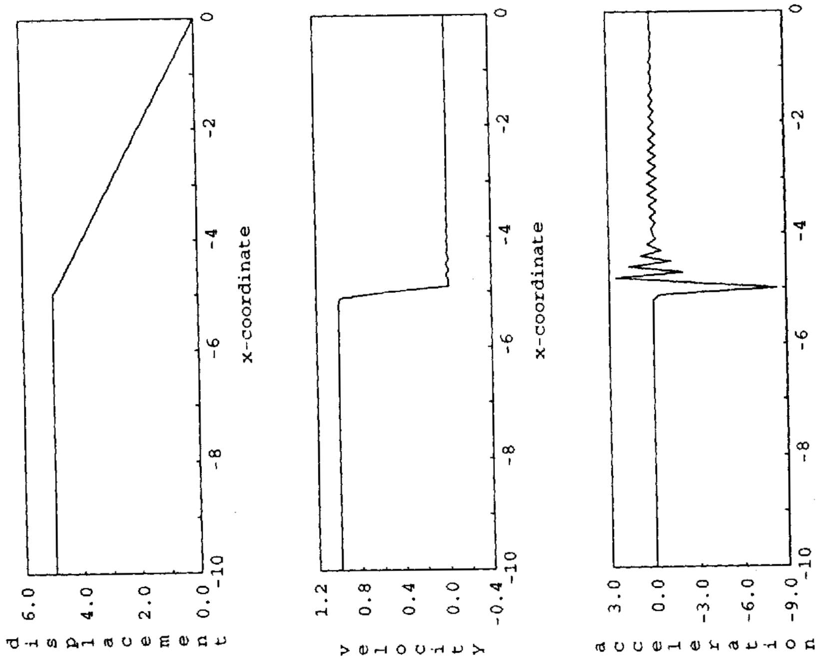

Figure 6. Bar on rigid wall; kinematic fields for $\beta = 0{\cdot}001$, $\gamma = 0{\cdot}5$

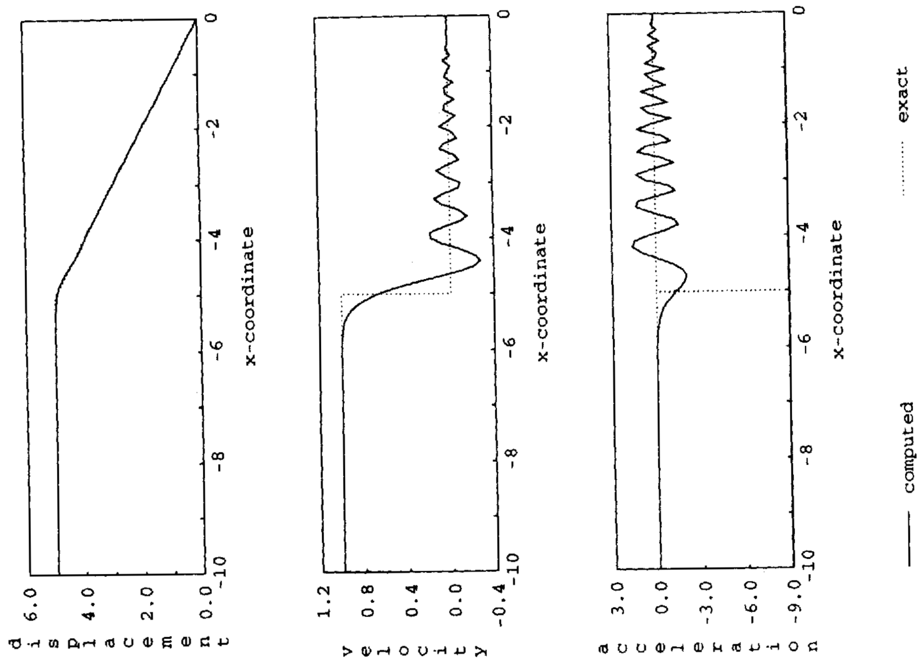

Figure 5. Bar on rigid wall; kinematic fields for $\beta = 0{\cdot}25$, $\gamma = 0{\cdot}5$

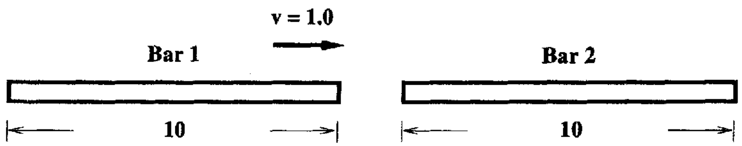

Figure 7. Impact of identical bars

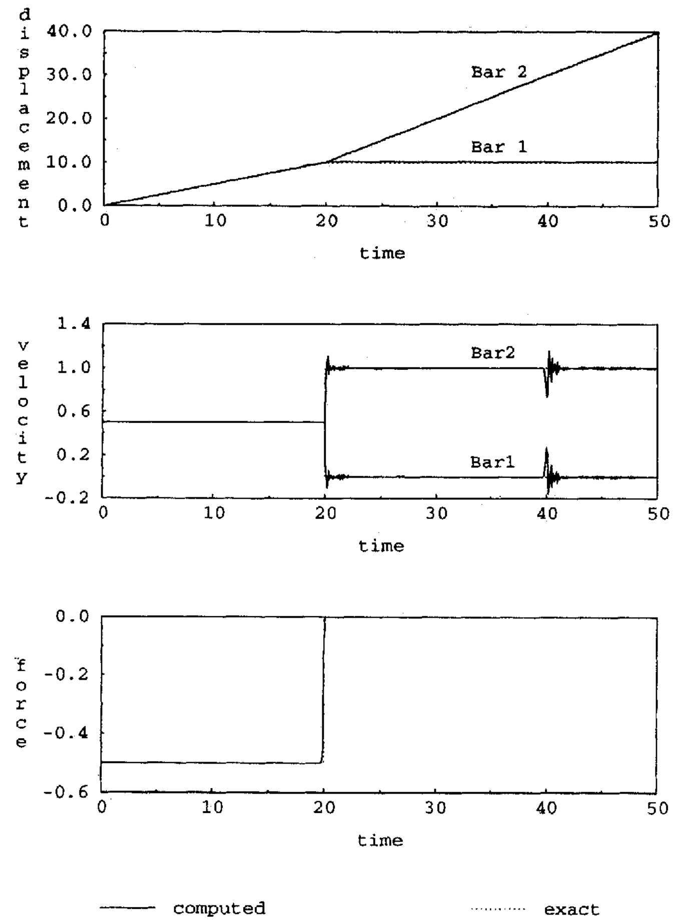

Figure 8. Impact of identical bars; history of tip displacements, velocities and contact force

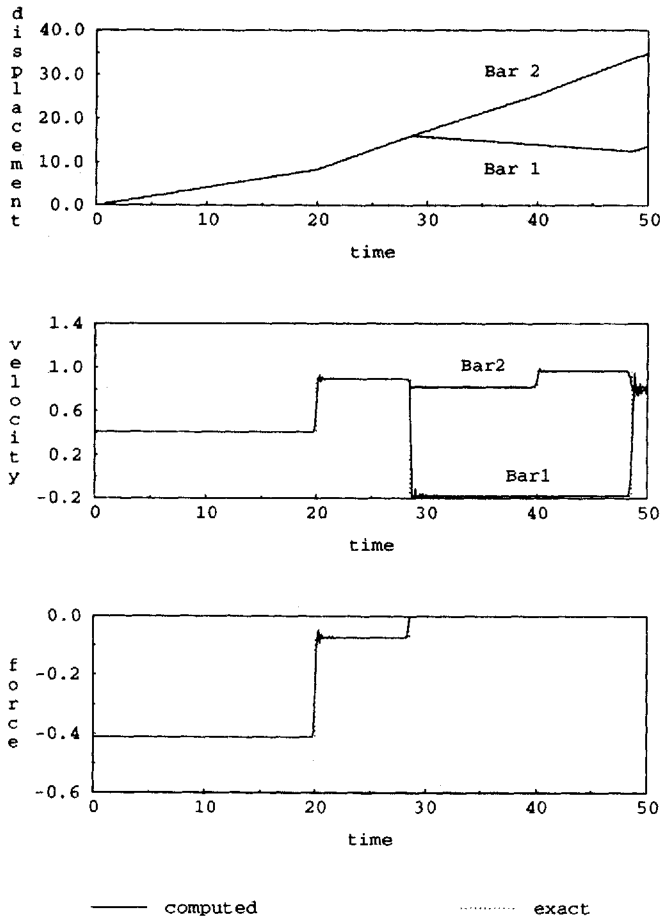

Figure 9. Impact of dissimilar bars; history of tip displacements, velocities and contact force

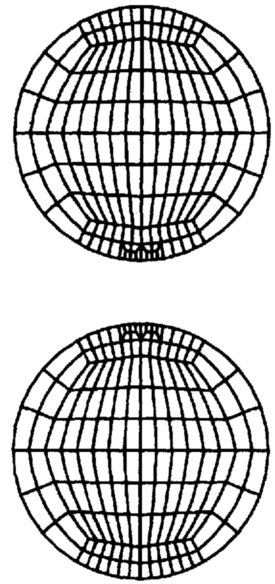

Figure 10. Impact of identical spheres; discretization

plotted in Figure 11 ($\rho = 1{\cdot}0, \Delta t = 0{\cdot}05$) and Figure 12 ($\rho = 0{\cdot}001, \Delta t = 0{\cdot}0025$), and is compared with the approximate Hertzian solution. As noted in Reference 12 (pp. 198–200), the Hertzian solution is 'static', in the sense that it neglects the effects of wave propagation. The ratio r of fundamental period for the dilatational wave to total impact time can be found to be

$$r \approx 1{\cdot}22\left(\frac{\|\mathbf{v}\|}{c}\right)^{0{\cdot}2}$$

where c is the speed of the dilatational wave. The validity of Love's argument that the Hertzian solution becomes more accurate as r decreases towards zero is confirmed by the numerical

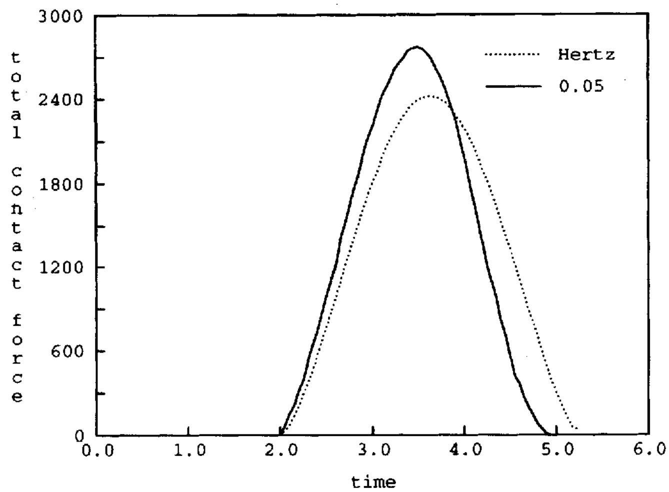

Figure 11. Impact of identical spheres; history of total contact force ($\rho = 1{\cdot}0$)

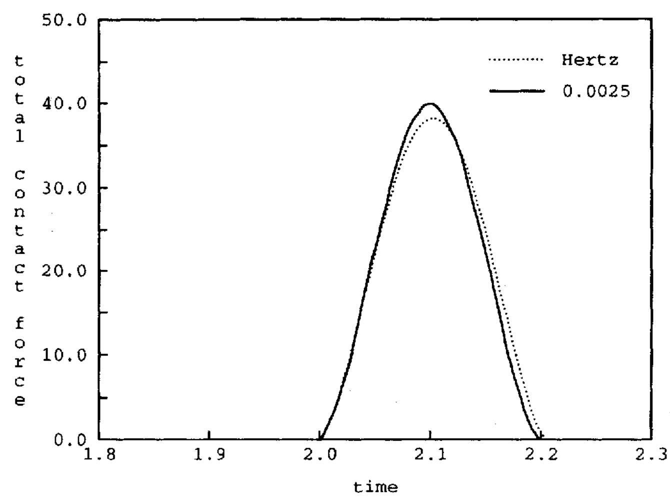

Figure 12. Impact of identical spheres; history of total contact force ($\rho = 0{\cdot}001$)

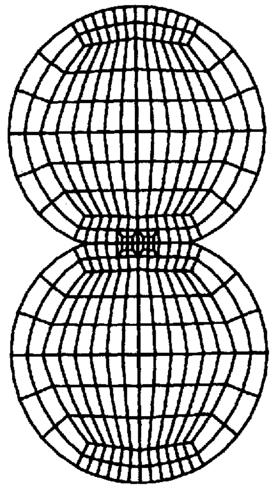

Figure 13. Impact of identical spheres; deformed meshes at $t = 3{\cdot}5$ ($\rho = 1{\cdot}0$)

solutions, since $r(E_s, \nu_s, \rho = 1{\cdot}0) \approx 0{\cdot}60$ and $r(E_s, \nu_s, \rho = 0{\cdot}001) \approx 0{\cdot}30$. Finally, a representative deformed mesh is shown in Figure 13.

7. CONCLUSIONS

In the context of semi-discrete time integrators it has been shown, in sharp contrast with the continuous case, that satisfaction of the impenetrability constraints is not sufficient, when simulating problems featuring persistent mechanical contact. A simple, efficient and widely applicable methodology, based on appropriate constraining of all boundary kinematic fields upon detection of contact, has been developed, that bypasses the above shortcoming and maintains overall consistency of time integration. Numerical simulations have demonstrated the merits of the proposed treatment.

ACKNOWLEDGEMENT

This work has been supported by the Lawrence Livermore National Laboratory under contract No. W-7405-ENG-48. The continuous interest of Dr. G. L. Goudreau of LLNL is especially acknowledged.

REFERENCES

1. T. F. Conry and A. Seireg, 'A mathematical programming method for design of elastic bodies in contact', *J. Appl. Mech.*, **38**, 387–392 (1971).
2. S. K. Chan and I. S. Tuba, 'A finite element method for contact problems of solid bodies—part I. Theory and validation', *Int. J. Mech. Sci.*, **13**, 615–625 (1971).
3. A. Francavilla and O. C. Zienkiewicz, 'A note on numerical computation of elastic contact problems', *Int. j. numer. methods eng.*, **9**, 913–924 (1975).
4. T. J. R. Hughes, R. L. Taylor, J. L. Sackman, A. Curnier and W. Kanoknukulchai, 'A finite element method for a class of contact–impact problems', *Comput. Methods Appl. Mech. Eng.*, **8**, 249–276 (1976).
5. W. R. Hamilton, 'On a general method in dynamics', *Phil. Trans. Roy. Soc. London*, **124**, 247–308 (1834).
6. W. R. Hamilton, 'Second essay on a general method in dynamics', *Phil. Trans. Roy. Soc. London*, **125**, 95–144 (1835).

7. P. Papadopoulos and R. L. Taylor, 'A mixed formulation for the finite element solution of contact problems', *Comput. Methods Appl. Mech. Eng.*, **94**, 373–389 (1992).
8. N. M. Newmark, 'A method of computation in structural dynamics', *J. Eng. Mech. Div. ASCE*, **85**, 67–94 (1959).
9. W. L. Wood, *Practical Time-stepping Schemes*, Oxford University Press, Oxford, 1990.
10. O. C. Zienkiewicz and R. L. Taylor, *The Finite Element Method; Basic Formulation and Linear Problems*, Vol. 1, 4th edn, McGraw-Hill, London, 1989.
11. O. C. Zienkiewicz and R. L. Taylor, *The Finite Element Method; Solid and Fluid Mechanics, Dynamics and Non-linearity*, Vol. 2, 4th edn, McGraw-Hill, London, 1991.
12. A. E. H. Love, *A Treatise on the Mathematical Theory of Elasticity*, 4th edn, Cambridge University Press, Cambridge, 1927.